CONCRETE LIBRARY OF JSCE NO. 36, DECEMBER 2000

A PREDICTION MODEL FOR TENSILE CREEP STRAIN OF CONCRETE BASED ON MICRO PORE BEHAVIOR

(Translation from Proceeding of JSCE, No.613/V-42, February 1999)


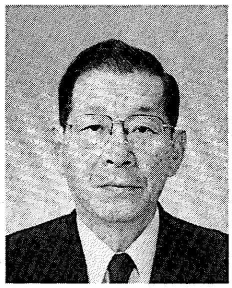
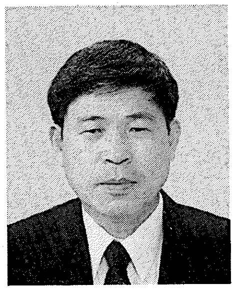
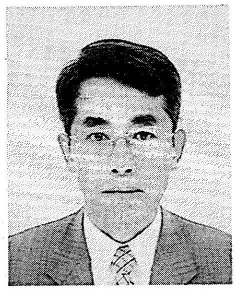

Tomoji KUMANO Shinzo NISHIBAYASHI Shoichi INOUE Akira YOSHINO

Tensile creep is an important characteristic of concrete that has an influence on crack behavior. In this paper, a prediction method for tensile creep strain based on the micro mechanism is proposed on the basis of observations of micro pore behavior under sustained tensile stress. A micro mechanical prediction model is developed. Using this model, the tensile creep strain of concrete under varying conditions of loading stress, loading age, and water-cement ratio is predicted correctly. With inspect to temperature effect, it is shown through a comparison with data in the past literature that this model may generally predict tensile creep strain of concrete.

Key Words : *tensile creep, pore structure, capillary pore, micro crack, linear fracture mechanics, stress dependent rate process*

Tomoji Kumano is a member of the Technology Department of the Civil Engineering Division at Shimizu Corporation, Japan. He obtained his D.Eng. from Tottori University in 1998. His research interests relate to the micro structure of concrete and deformation mechanism. He is a member of the JSCE.

Shinzo Nishibayashi is a Professor in the Department of Civil Engineering at Osaka Sangyo University. He obtained his D.Eng. from Kyoto University in 1968. His research interests include the properties of fresh concrete, the alkali silica reaction, and the repair of concrete structures. He is a member of the JSCE.

Syouichi Inoue is a Professor in the department of Civil Engineering at Tottori University. He obtained his D.Eng. from the University of Kyoto in 1985. His research interests include the fatigue properties, time-dependent deformation of concrete structures, and properties of fresh concrete. He is a member of the JSCE.

Akira Yoshino is an Associate Professor in the department of Civil Engineering at Tottori University. He obtained his D.Eng. from the University of Nagoya in 1994. His research interests relate to the properties of fresh concrete and construction. He is a member of the JSCE.

1. INTRODUCTION

Through investigations, the compressive creep behavior of concrete has clarified. The results of these studies have been arranged systematically, and some prediction equations for use in design have been proposed [1]. In contrast, few investigations of tensile creep behavior have been carried out, since in reinforced concrete structures, the concrete resists compressive forces and the reinforcing bars takes the tensile load. As a result, no understanding of the tensile creep behavior of concrete. However, tensile creep is an important factor influencing the crack behavior of concrete. Recently, with concrete structures such as a nuclear power plants and storage plants becoming extremely large and high performance, some studies of tensile creep in concrete aimed at predicting the crack behavior of concrete have been published [2].

In the usual design method for concrete structures, compressive creep properties are treated under tensile stress, according to the Davis-Glanville law. However, in a recent study [3], it is indicated that the creep strain and the mechanism of creep differ between compressive loading and tensile loading. Therefore, in order to understand the tensile creep properties and to clarify how tensile creep strain may be predicted, it is important to discuss tensile creep behavior based on its actual mechanism.

On the other hand, in the performance based design method[4], which is being discussed as the design method of the next generation, concrete structures will need to be designed such that the required performance is satisfied on the time axis using behavior- predicting technologies. In this design method, predicting the behavior of the structure under various conditions on the time axis is more important than an index indicating whether the structure is safe or not. To acieve this, the development of prediction methods based on an understanding of micro mechanisms will be necessary.

To this end, in order to develop a prediction model for tensile creep strain based on the micro mechanisms at work, an observation of the micro pore behavior of concrete under sustained tensile stress is carried out and a micro mechanical prediction model is organized. Still more, the prediction model is verified. This paper reports on the results of this effort.

2. EFFECT OF SUSTAINED TENSILE STRESS ON PORE STRUCTURE OF CONCRETE

A prediction method for tensile creep strain based on the underlying micro mechanisms requires that the micro pore behavior of concrete under sustained tensile stress be expressed mathematically. Therefore, observations of micro pore behavior under sustained tensile loading is the first step toward development of an accurate prediction model. To achieve this, the distribution of micro pore diameters in concrete was measured using a pressured mercury porosimeter, and the results under sustained tensile stress were compared with these for concrete under no stress.

2.1 Experimental Program

a) Materials and mix proportions
Normal Portland cement (density : 3.15 g/cm^3; blaine value : 3150 cm^2/g) was used in this investigation. The coarse aggregate was crushed stone (density : 2.69 g/cm^3; F.M. : 6.51), and the fine aggregate was a mixture of crushed sand and natural sand (density : 2.67 g/cm^3, F.M. : 2.79). Table 1 shows the mix proportion.
b) Manufacture of specimens

Table 1 Mix Proportion of Concrete

Type of cement	G_{max} (mm)	Slump (cm)	Air (%)	W/C (%)	s/a (%)	Unit weight(kg/m^3) W	C	S	G	ad. C×%
Normal	20	8±1	4.5±1	50	44.5	157	314	821	1041	0.25

ad.:Air-entraining admixture

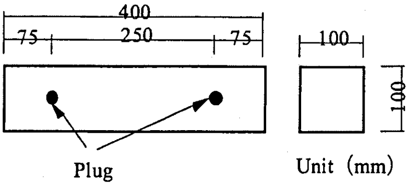

* Specimens are sealed with alminium tape

Fig. 1 Outline of Specimen

Table 2 Summary of Test Program

Loading age (day)	Loading stress (N/mm²)	Stress/ strength ratio	Loading duration (day)	Temp. (℃)	Humidity (%)
3	0.8	0.29	0	20	100 (Sealed)
	1.2	0.52	7		
	1.6	0.63	28		

Test series : N-50-3-0.8

- 0.8 — Loading stress (N/mm²)
- 3 — Loading age (day)
- 50 — W/C(%)
- N — Normal cement

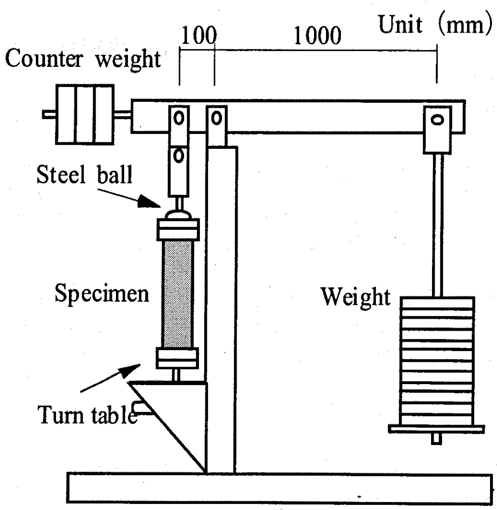

Fig. 2 Outline of Test Machine

Concrete was mixed using a pan-type forced-action mixer with a capacity of 100 liters. One batch of concrete was 70 liters. The target slump value and air content were 8 cm and 4.5%, respectively. The temperature of the freshly mixed concrete was adjusted to 20℃. An outline of specimen is shown in Fig.1. Six test specimens measuring 10×10×40 cm were cast for each test factor, and three being loaded and others left loaded. At same time, column specimens were cast for compressive strength testing. After demolding the next day, prism specimens were placed in 20℃ water for 24 hours, after which the specimen surface was wiped dry and sealed with aluminum tape to maintain 100% absorption. The weight of these sealed prism specimens was confirmed to be constant till 28 days. These prism specimens were placed in a room until testing.

c) Experimental method
Table 2 gives a summary of the test program and the explains specimen nameing. The loading age was three days, and the loading stresses were 0.8, 1.2, and 1.6 N/mm^2, giving loading stresses per tensile strength of 0.29, 0.52, and 0.63, respectively. Tensile creep tests were carried out using three-lever type equipment with a lever ratio of 10 : 1 (Fig.2).

The specimen was fixed to the test equipment an epoxy resin bonding agent. A pair of point gauges was fixed to each side of the specimen, except for the faces at which stress was applied. Strain was measured using a Whittemore strain meter with a minimum division of 1/1000 mm at 12-hour intervals until three days from loading and at 24-hour intervals afterward. Loading periods were 0 (instantaneous loading), 7, and 28 days. The loaded and non-loaded specimens were divided into four parts longitudinally, and the center parts were crushed. After sampling the 2.5-5mm particles from each crushed part, the samples were preserved in acetone and made D-dry for 48 hours, after which the micro pore depth distributions of samples were measured using a pressured mercury porosimeter.

2.2 Test Results and Discussion

Table 3 shows the properties of the fresh concrete and the mechanical properties of the hardened concrete. Figure 3 shows the results of tensile creep strain as corrected by the strain of an unstressed specimen. The tensile strain increased with increasing loading stress.

a) Effect of sustained tensile stress on micro pore diameter distributions
Figure 4 shows the micro pore diameter distributions at 0 (instantaneous loading), 7, and 28 days, and also the results for the unloaded specimen. Here, the range of micro pore diameter is divided into the following ranges according to distribution shape, in order to carry out a detailed comparison:

Table 3 Test Results

Test series	Slump (cm)	Air (%)	Temp. (℃)	age (day)	Compressive strength (N/mm^2)	Compressive Young's modulus (kN/mm^2)	Splitting tensile strength (N/mm^2)
N-50-3-0.8	6.0	3.5	25.0	3	24.6	30.1	2.73
				10	35.5	33.5	3.17
				31	46.9	35.4	3.39
N-50-3-1.2	11.5	3.8	20.0	3	21.1	24.9	2.31
				10	35.0	34.8	3.00
				31	44.4	38.1	3.61
N-50-3-1.6	7.5	4.0	19.0	3	23.7	26.9	2.54
				10	31.3	32.2	2.62
				31	43.5	36.2	3.54

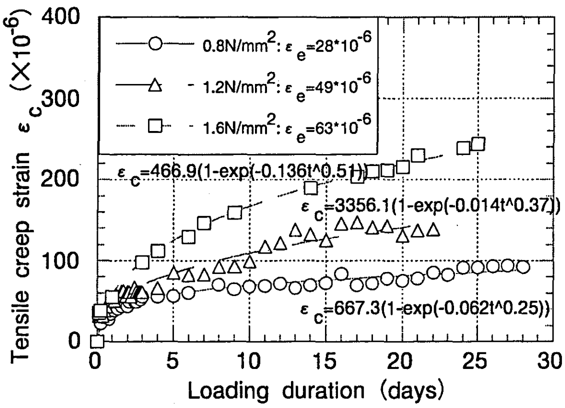

Fig. 3 Tensile Creep Test Results

① From 0.003 to 0.01 μ m, which peaks at about 0.005 μ m.
②From 0.01 to 0.1 μ m, which peaks at 0.03 ~ 0.07 μ m.
③ From 0.1 to 5 μ m, at which the distribution is gently sloping and the micro pore volume disappears.
④ Above 5 μ m, at which the micro pore volume appears again.

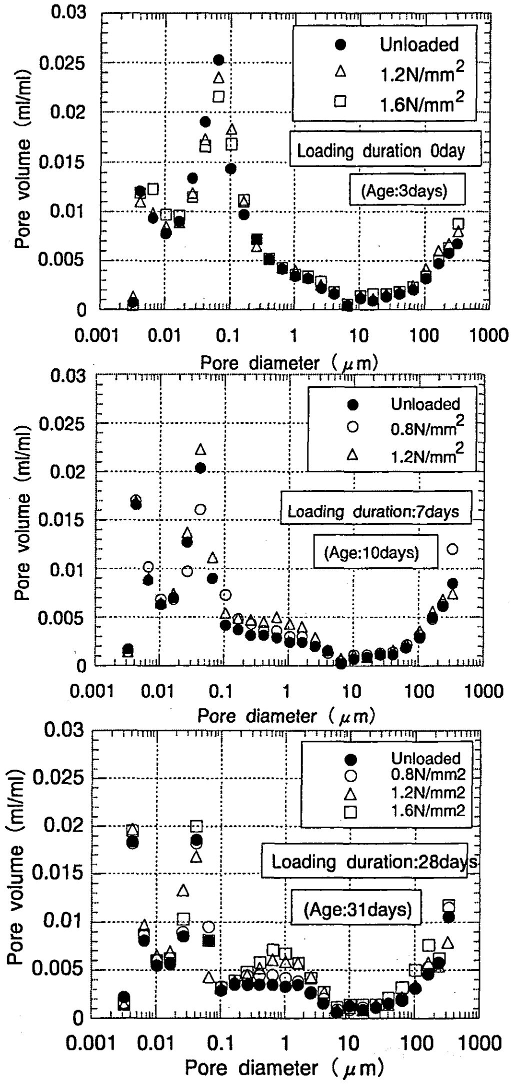

Fig. 4 Pore Diameter Distribution

For the unloaded specimen, the micro pore volume from 0.003 to 0.01 μ m increased with elapsed time and that from 0.01 to 0.1 μ m, where the peak shifted from 0.07 to 0.03 μ m, decreased. It is thought that this behavior reflects a reduction in micro pore diameter with hydration. The decrease in micro pore volume from 0.1 to 5 μ m, which decreased at about 0.1 μ m pore diameter, was less than that from 0.01 to 0.1 μ m, particularly from 7 days form 28 days of age. The micro pore volume above 5 μ m was constant. It is thought that the micro pore volume in this range corresponds to the entrained air [6].

These micro pore diameter distributions under sustained tensile stress were compared with those of unstressed concrete. The micro pore volume from 0.1 to 5 μ m under sustained tensile stress is greater than that under no stress. This tendency was particularly notable with increasing loading period and loading stress. Therefore, it is thought that sustained tensile stress causes an increase in micro pore volume from 0.1 to 5 μ m. Uchikawa et al reported that micro pores from 0.1 to 5 μ m are capillary pores in the transition zone, and these capillary pores are thought to be points at which micro cracks occur [7]. Tanaka et al have reported that, in an investigation of tensile creep in concrete at an early age, the acoustic emission activity (event counts), which reflects the occurrence of micro cracks, increased with increasing the loading stress. From these reports, it is thought that the increase in micro pore volume in this range under sustained tensile stress must be due to micro cracks occurring and developing.

b) Relationship between micro pore volume and tensile creep strain

In order to examine the relationship between micro pore volume change in each diameter range and tensile

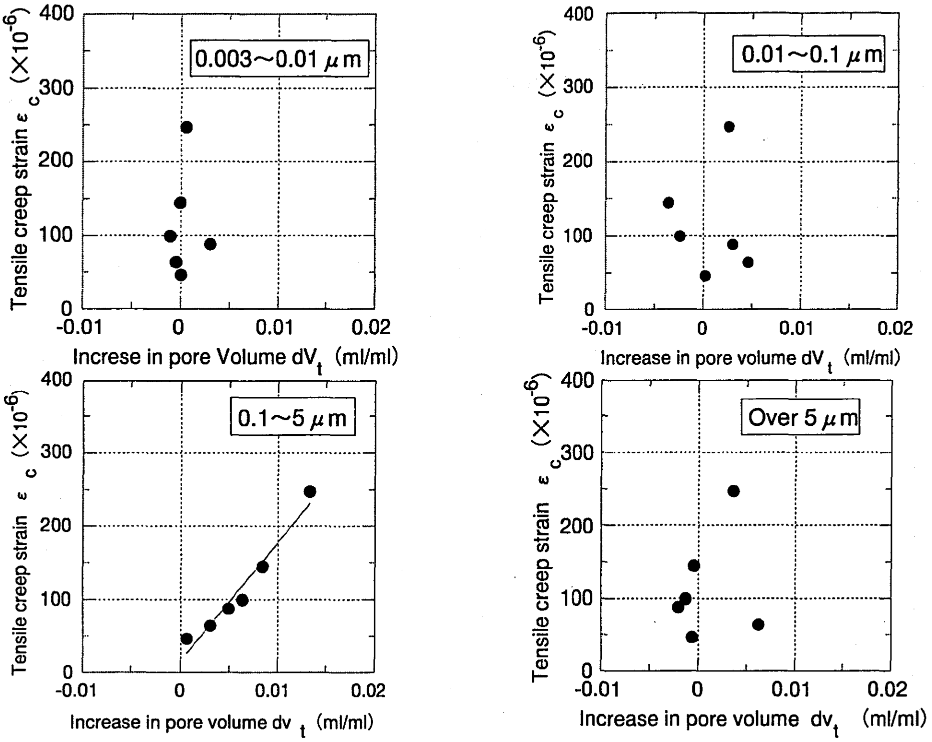

Fig. 4 Relationship between Increase in Pore Volume and Creep Strain

creep strain, the increase $dV_{t-t'}$ is defined as follows,

$$dV_{t-t'} = V_{c,t-t'} - V_{n,t-t'} - dV_{t'} \tag{1}$$

where, $V_{c,t-t'}$ is the micro pore volume of the range in question in a specimen stressed time t to t'; $V_{n,t-t'}$ is the micro pore volume of the range in question in an unstressed specimen kept in the same environment as the stressed specimen t to t'; and $dV_{t'}$ is the difference in micro pore volume of the range in question between the immediately unloaded specimen and the unstressed specimen at $_{t'}$.

Figure 5 shows the relationship between increase in micro pore volume ($dV_{t-t'}$) and tensile creep strain. The relationship is linear for the 0.1 to 5 μ m range of micro pore (relative coefficient r=0.983) , though the other relationships are unclear.

If the increase in micro pore volume in the 0.1 to 5 μ m range is due to the micro cracking and crack development, this linear relationship indicates that micro crack development may be related to the tensile creep strain by a suitable linear theory. In the next chapter, an attempt is made to develop a model based on the concept of linear fracture mechanics.

3. PREDICTION MODEL FOR TENSILE CREEP STRAIN BASED ON MICRO CRACK DEVELOPMENT

3.1 Assumptions

The method used to predict tensile creep strain is a model based on micro cracks occurring and developing at capillary pores. Consequently the shape, size, and spatial distribution of capillary pores must be considered. Also, changes in capillary pore distribution with hydration and the development of micro cracks with time must be considered. However it is very difficult to faithfully model the pore structure in concrete, which changes with space and time. Further, the simplest possible model is desired in the engineering field. Thus, based on the following assumptions, an attempt is made to present a simple model based on an easy mathematical treatment:

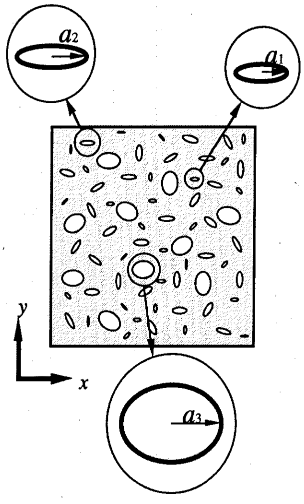

Fig. 6 Modeling of Micro Pore Structure in Concrete

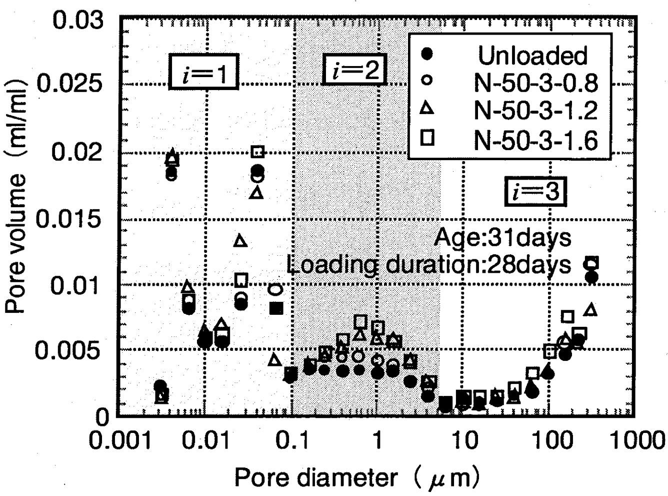

Fig. 7 Concept of Range in Elliptic Cracks

① The pore structure is isiotropic in space.
② The pore structure is homogeneous in space.
③ The concrete is saturated.
④ The development of hydration is expressed as a decrease in the number of pores.
⑤ A small yield area forms around the end of a crack as it develops from a pore.

Assumption ④ is the mathematical expression of changes in pore structure with hydration. It is known that the pore volume in concrete decreases with age[9], and it is thought that this is because hydrates fill the pores as hydration proceeds. In this paper, in order to simplify our model mathematically, the decrease of micro pore volume with hydration is expressed as a decrease in the number of pores.

Figure 6 shows the resulting two-dimensional model of the pore structure of concrete. There is a random distribution of elliptic cracks of longitudinal radius a_1, a_2, and a_3 in quantities $\rho_1(t)$, $\rho_2(t)$,and $\rho_3(t)$, respectively. These three crack sizes are typical micro pore radii taken from the results of observations of micro pore volume distributions, with a_1 being the typical micro pore longitudinal radius for pores under 0.1 μm, a_2 for pores from 0.1 to 5 μm in which the micro pore volume increases under sustained tensile stress, and a_3 for pores above 5 μm which are thought to correspond to the entrained air (Fig 7).

It is thought that the determined tensile creep strain results from a decrease in elliptic cracks with hydration and the development of cracks from elliptic cracks in the two-dimensional plane shown in Fig. 6.

3.2 Increase in Tensile Creep Strain Based on Development of Micro Crack [10]

It is assumed that all elliptic cracks in the two-dimensional plane shown in Fig. 6 are oliented to the x-axis at an angle of θ [11]. When this plane is loaded by stress σ_j (i.e. σ_x, σ_y, τ_{xy}), the normal stress p and shearing stress q on the plane parallel to the crack are given by equation (2).

$$\begin{aligned} p &= \sigma_x \sin^2\theta + \sigma_y \cos^2\theta - \tau_{xy} \sin 2\theta \\ q &= -\sigma_x \sin\theta\cos\theta + \sigma_y \sin\theta\cos\theta + \tau_{xy}\cos 2\theta \end{aligned} \tag{2}$$

Figure 8 shows the strain energy density and the method of calculating tensile creep strain, where, W_{0j} is the strain energy density at $a_i = 0$; ε_{0j} is the strain at $a_i = 0$; $\Delta W_{e,i,j}$ is the increase in strain energy density due to the three types of elliptic crack (i=1, 2,and 3) ; and $\Delta\varepsilon_{e,i,j}$ is the increase in strain due to the three types of elliptic crack (i=1, 2, and 3). When a crack develops from an elliptic crack, the increase in strain energy density and strain are $\Delta W_{c,i,j}(t-t')$ and $\Delta\varepsilon_{c,i,j}$, respectively. The strain energy density W_{ij} and the strain $\varepsilon_{i,j}$ are given by equation (3).

$$\begin{aligned} W_{i,j} &= W_{0,j} + \Delta W_{e,i,j}(t) + \Delta W_{c,i,j}(t-t') \\ \varepsilon_{i,j} &= \varepsilon_{0,j} + \Delta\varepsilon_{e,i,j}(t) + \Delta\varepsilon_{c,i,j}(t-t') \end{aligned} \tag{3}$$

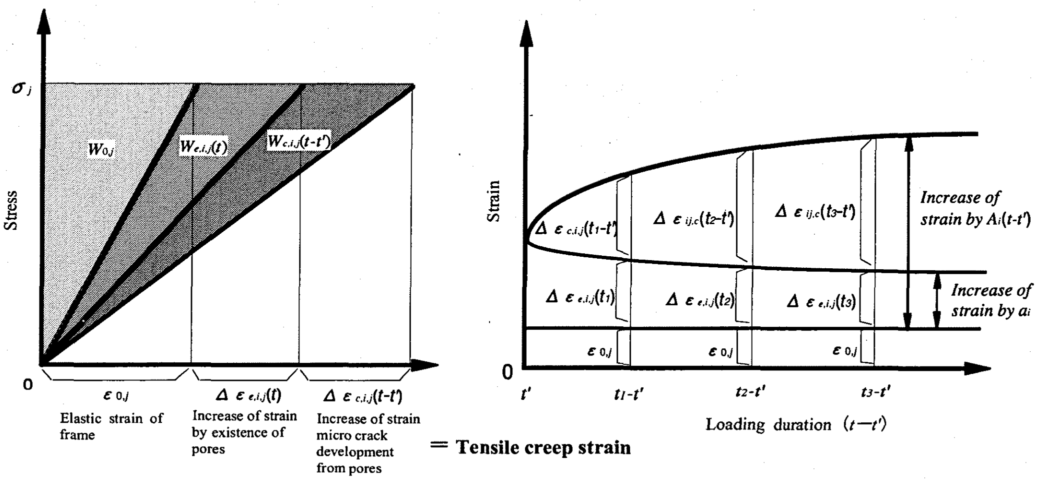

Fig. 8 Concept of Strain Energy Density and Tensile Creep Strain

The relationship between strain energy density and the ratio of energy release is given by equation (4).

$$\frac{\partial W_{i,j}}{\partial(2a_i)} = \zeta_{i,j} \tag{4}$$

When the longitudinal radius of cracks develops from ai to $A_i(t-t')$, the strain energy density increase is given by equation(5).

$$\Delta W_{c,i,j}(t-t') = \rho_i(t)\int_{a_i}^{A_i(t-t')} \zeta_{i,j}(2da_i) \tag{5}$$

Therefore, the sum of strain energy density increase for the three types of cracks is,

$$\sum_{i=1}^{3}\Delta W_{c,i,j}(t-t') = \sum_{i=1}^{3} \rho_i(t)\int_{a_i}^{A_i(t-t')} \zeta_{i,j}(2da_i) \tag{6}$$

Now, it is assumed that there is no mutual intereference, so the stress intensity factors $K_{I,i,j}$ and $K_{II,i,j}$ are given by equation (7).

$$K_{I,i,j} = p\sqrt{\pi a_i} \quad , \quad K_{II,i,j} = q\sqrt{\pi a_i} \tag{7}$$

The relation between energy release rate and stress intensity factor is then given by equation (8).

$$\zeta_{i,j} = \frac{K_{I,i,j}{}^2}{E'} + \frac{K_{II,i,j}{}^2}{E'} \tag{8}$$

Equations (7) and (8) are substituted for equation (6), to give,

$$\sum_{i=1}^{3}\Delta W_{c,i,j}(t-t') = \sum_{i=1}^{3}\frac{\pi\left[A_i(t-t')^2 - a_i{}^2\right]\rho_i(t)}{E'} \times \left[f_I(p)p^2 + q^2\right] \tag{9}$$

Consequently, the sum of strain increase as the three types of cracks develop is given by equation (10).

$$\sum_{i=1}^{3}\Delta\varepsilon_{c,i,j}(t-t') = \sum_{i=1}^{3}\frac{\partial\Delta W_{c,i,j}(t-t')}{\partial\sigma_j} = \sum_{i=1}^{3}\frac{2\pi\left[A_i(t-t')^2 - a_i{}^2\right]\rho_i(t)}{E'}\left[f_I(p)p\frac{\partial p}{\partial\sigma_j} + q\frac{\partial q}{\partial\sigma_j}\right] \tag{10}$$

It is assumed that the elliptic cracks that model capillary pores are distributed at random. Further, it is assumed that distribution function is uniform, g(θ)=1/ π . In this study, the strain increase under uniaxial tensile stress is considered, so the applied stress is simply σ_y. Namely

$$\sum_{i=1}^{3}\Delta\bar{\varepsilon}_{c,i,y}(t-t') = \sum_{i=1}^{3}\int_{-\frac{\pi}{2}}^{\frac{\pi}{2}} g(\theta)\Delta\varepsilon_{c,i,y}(t-t')d\theta = \sum_{i=1}^{3}\frac{\pi\left[A_i(t-t')^2 - a_i{}^2\right]\rho_i(t)}{E'}\sigma_y \tag{11}$$

Equation (11) is a generalized equation for the case where micro cracking development is the main mechanism of creep under sustained tensile stress. On the other hand, an increase in capillary pore volume is observed only for pore diameters from 0.1 to 5.0 μ m (i=2). Thus, equation (11) is simplized to equation (12).

$$\Delta\bar{\varepsilon}_{c,2,y}(t-t') = \frac{\pi[A_2(t-t')^2 - a_2{}^2]\rho_2(t)}{E'}\sigma_y \qquad (12)$$

3.3 The Micro Cracking Development Law

The micro cracking development law $A_2(t\text{-}t')$ and the change in capillary pore count $\rho_2(t)$ accompanying hydration are incorporated into equation (12). Studies of change in micro structure become common as a boundary area between cement chemical and concrete engineering, but the effot has not been organized sufficiently. Then we may lead $\rho_2(t)$ by measurering pore diameter distribution of unstressed specimen which cured similar to stressed specimen. On the other hand, the prediction of a micro cracking law is a very important part of this study. Consequently, we adopt a mechanical approach and attempt to apply rate process theory.

The rate process theory which is applied to the fracturing of solid materials and determination of crack growth rate is also known as stress-dependent rate process theory. The concept is shown in Fig.9. When no stress is applied, the height of the energy wall when the process is travelling toward the right along the reaction axis is similar to that when travelling toward the left. In this case, the reaction does not proceed in either direction. When a stress, σ, is applied, the energy wall is lower at $\phi(\sigma)$ in one direction as compared with the other. As a result the process moves toward decreasing potential energy at a certain rate. The rate is given by equation (13).

$$r = \frac{kT}{h}\exp[-(\Delta F - \phi(\sigma))/kT] \qquad (13)$$

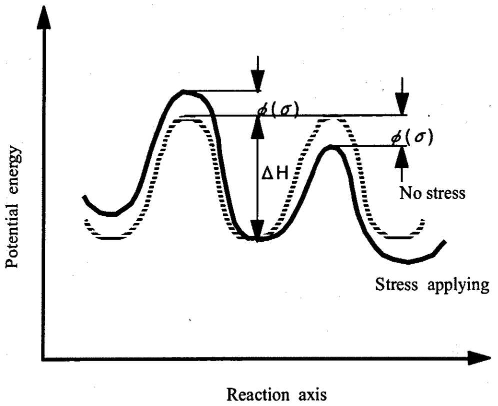

Fig. 9 Concept of Stress-dependent Rate Process Theory

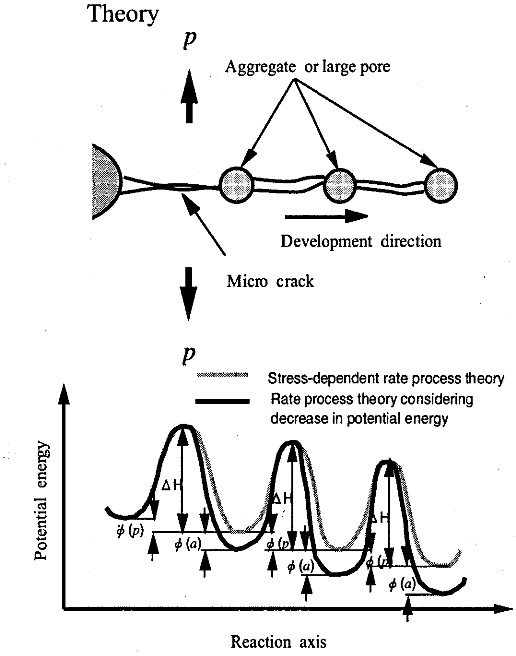

Fig. 10 Stress-dependent Rate Process Theory Considering Decrease in Free Energy

where, k is Boltzman's constant (=1.38 × 10^{-23}J/K); h is Plank's constant (=6.62 × 10^{-34}Js); T is absolute temperature (K) and Δ F is free active energy (J).

Mitsuhashi[13] assumed that concrete was a brittle material containing many pores and then showed a crack growth rate that was adapted for the reliable analisys in fractures as equation (14).

$$r = \frac{kT}{h}\exp\left[-(\Delta F - \frac{1}{n_b}\ln\alpha\sigma)/kT\right] \qquad (14)$$

where, nb is the number of atoms in the crack tip to applied high concentrated stress, and α is the proportional constant between stress and the energy wall height.

Equation (14) is adapted for brittle fractures in which the macro cracks grow rapidly and extend to fractures. When a creep fracture is not occured, it is considered that micro cracks grow intermittently as a result of the crack arresting effect of aggregates and large pores [14]. As a result, the free active energy will decrease through a surface energy increase as cracks develop, and the average rate of crack development will decrease slowly. Namely, when the average rate of micro crack development is disccussed, the decrease in free active energy must be considered.

The stress-dependent rate process theory modified to take account of this decrease in free energy is illustrated in Fig.10. The increase in surface energy, W_a, with crack development is given by equation (15).

$$W_a = 2\eta a \tag{15}$$

where, η is surface energy per unit crack length and a is longitudinal radius of elliptic cracks.

If it is assumed that $\phi\ (a)$ is given by a logarithmic function similar to $\phi\ (\ \sigma\ )$, the effect of a surface energy increase is represented logarithmic function, and the rate of crack growth is given by equation (16).

$$r = \frac{kT}{h}\exp\left[-(\Delta F - \frac{1}{n_1}\ln \alpha p + \frac{1}{n_2}\ln 2\eta a)/kT\right] \tag{16}$$

where, n_1 is number of atoms in the crack tip applied high concentrated stress and n_2 is the number of atoms that release energy with crack development.

It is assumed that the rate of crack growth is proporsitional to the micro crack development rate.

$$\frac{da}{dt} = C\frac{kT}{h}\exp\left[-(\Delta F - \frac{1}{n_1}\ln \alpha p + \frac{1}{n_2}\ln 2\eta a)/kT\right] = \beta(\alpha p)^{\frac{1}{n_1 kT}}(2\eta a)^{\frac{-1}{n_2 kT}} \tag{17}$$

where, $\beta = C\frac{kT}{h}\exp\left(-\frac{\Delta F}{kT}\right)$ and C is constant of proportionality.

Therefore $A_2(t\text{-}t')$ is given by equation (18).

$$A_2(t-t') = \left[(1+\frac{1}{n_2 kT})\beta(\alpha p)^{\frac{1}{n_1 kT}}(2\eta)^{\frac{-1}{n_2 kT}}(t-t')\right]^{\frac{1}{1+\frac{1}{n_2 kT}}} + a_2 \tag{18}$$

4.DETERMINING THE COEFFICIENTS IN THE PREDICTION MODEL

The prediction process using the proposed model is outlined in Fig.11. The following coefficients must be determined in order to predict tensile creep:

a_i:Size of ellipsed crack in the diameter range i (i=1,2,3)

E': Young's modulus of elastic frame

$\rho_i(t)$: Change in capillary pore count with hydration

α : Constant of proportionality between stress and energy wall height

$\beta(= C\frac{kT}{h}\exp\left(-\frac{\Delta F}{kT}\right))$:Constant of proportionality for change in temperature

η :Surface energy per unit crack length

n_1:Number of atoms in the crack tip applied high concentrated stress

n_2:Number of atoms releasing energy with crack development

The process for determining each of these coefficients is given below.

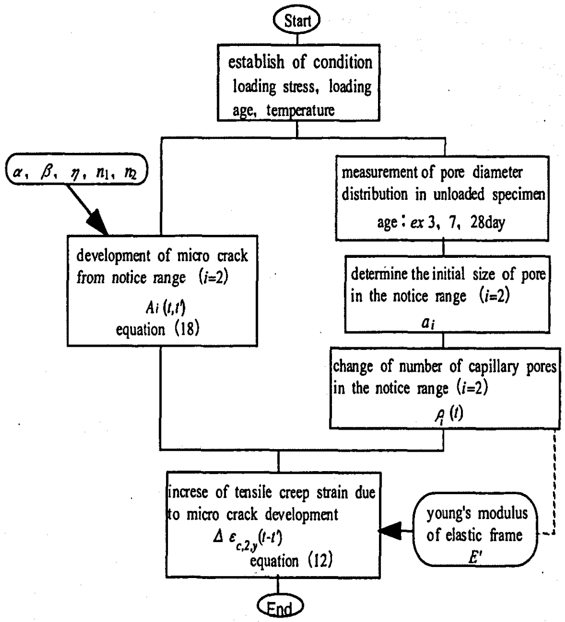

Fig. 11 Prediction of Tensile Creep Strain

4.1 Assumption of a_i

The typical size of capillary pores in each range is half the longitudinal radius of the elliptic crack

Table 4 Test Results

age (day)	Specimen / Range i	(μm)	N-50-3-0.8 Pore volume $V_i(t)$ (m^3/m^3)	N-50-3-0.8 Young's modulus E^* (kN/mm^2)	N-50-3-1.2 Pore volume $V_i(t)$ (m^3/m^3)	N-50-3-1.2 Young's modulus E^* (kN/mm^2)	N-50-3-1.6 Pore volume $V_i(t)$ (m^3/m^3)	N-50-3-1.6 Young's modulus E^* (kN/mm^2)
3	1	~0.1	0.0722	30.1	0.0648	24.9	0.0648	26.9
	2	0.1 ~5.0	0.0073		0.0114		0.0114	
	3	5.0~	0.0350		0.0380		0.0400	
10	1	~0.1	0.0606	33.5	0.0517	34.8	—	—
	2	0.1 ~5.0	0.0017		0.0028		—	
	3	5.0~	0.0350		0.0380		—	
31	1	~0.1	0.0466	35.4	0.0468	38.1	0.0467	36.2
	2	0.1 ~5.0	0.0039		0.0040		0.0040	
	3	5.0~	0.0350		0.0380		0.0400	

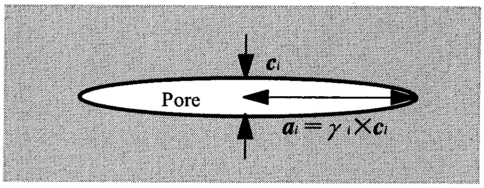

Fig. 12 Assumption of Pore Size

Table 5 Analysis Results

E' (kN/mm^2)	γ_1	γ_2	γ_3
58.7	18.5	112	1.54

that models the pore. In this study, information on pore size comes from the measurements by pressured mercury porosimeter. The pore diameter measured by porosimeter is the minimum distance between pore walls. Namely, the pore diameter measured by the porosimeter is not directly connected with a_i in the model. Thus, it is assumed that following relation exists between a_i and pore diameter c_i as measured by the porosimeter:

$$a_i = \gamma_i \times c_i \tag{19}$$

4.2 E' and γ_i

If it is assumed that the change in Young's modulus (apparent Young's modulus) measured by a uniaxial compressive test in a concrete specimen is caused by the change in pore volume as hydration progresses, a study based on fracture mechanics is impossible. The apparent Young's modulus at age t is given by adding elastic strain ε_{0j} to the strain increase $\varepsilon_{e,i,j}(t)$ that is caused by existence of pores. So the apparent elastic strain is given by equation (20).

$$\sum_{i=1}^{3} \varepsilon^*_{i,j}(t) = \varepsilon_{0,j} + \sum_{i=1}^{3} \Delta\varepsilon_{e,i,j}(t) \tag{20}$$

The integration range is from 0 to a_i. When a uniaxial compressive stress is applied to a specimen, $f_i(p)=0$ in the equation (9). The strain increase caused by existence of pores is given by an equation similar to equation (11).

$$\sum_{i=1}^{3} \Delta\varepsilon_{e,i,y}(t) = \sum_{i=1}^{3} \frac{\pi a_i^2 \rho_i(t)}{4E'} \sigma_y' \tag{21}$$

Equation (20) is substituted for equation (21), then $E^*(t)$ is given by equation (22).

$$E^*(t) = \frac{E'}{1 + \sum_{i=1}^{3} \frac{\pi a_i^2 \rho_i(t)}{4}} \tag{22}$$

where $V_i(t)$ is the pore volume in each range i in the unstressed specimen measured by pressured mercury porosimeter. Then equation (22) is written as equation (23).

$$E^*(t) = \frac{E'}{1 + \sum_{i=1}^{3} \frac{\gamma_i V_i(t)}{2}} \tag{23}$$

The unknowns in equation (23) are four. With four pair of data, $E^*(t)$, $V_i(t)$, E', and γ_i may be determined. The test results of $E^*(t)$ and $V_i(t)$ are shown as Table 4. E' and γ_i determined by equation (23) are shown as Table (5).

Soroka et al [15] reported that E' is about 90kN/mm^2 from experimental evaluation of cement paste. On the other hand, according to several assumptions in this study, E' is 58.7kN/mm^2. This is two thirds of Soroka's result. It is considered that this discrepancy is caused by following. Soroka et al evaluated E' from pore

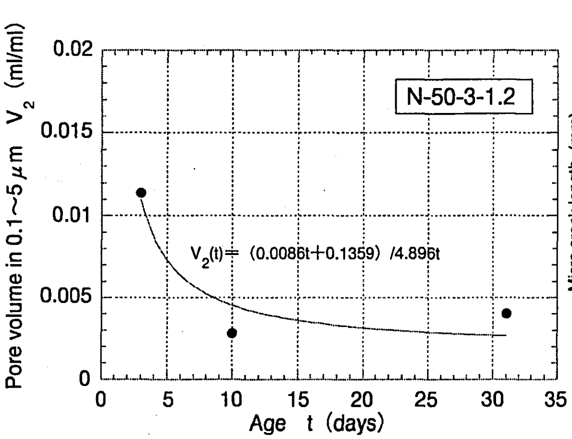

Fig. 13 Time-dependent Change in Pore Volume

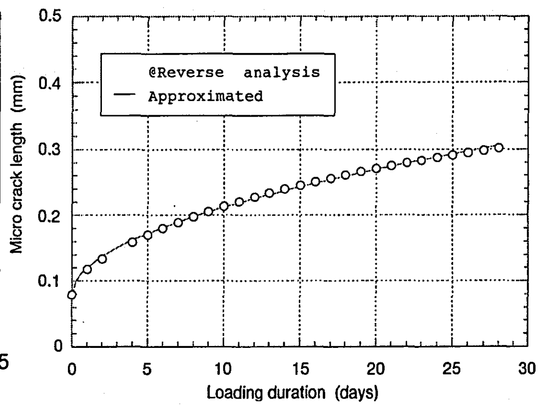

Fig. 14 Reverse Analysis of A2(t-t')

Table 6 Input Values

	Coeffcient	Value
Input	σ_y (N/mm^2)	1.2
	a_2 (mm)	0.0792
	γ_2	112
	E' (kN/mm^2)	58.7

Table 7 Determined Values

	Coeffcient	Value
Determined	α (J/N/mm^2)	0.0029
	β (1/s)	0.1955
	η (J/mm^2)	5.0368
	$\frac{1}{n_1 kT}$ (1/J)	0.4850
	$\frac{1}{n_2 kT}$ (1/J)	0.9398

volume in all range of cement paste. In this study, E' is evaluated from concrete including aggregates which have various Young's moduli. Moreover the evaluation range of pore diameter in this study is from 3nm to 300 μ m, this is different from pore volume in all range of Soroka's study.

γ_i is a coefficient that is expresses the shape of pores in each range i. The larger γ_i is, the flatter the pores. With γ_i equal to 0.5, the pores are circular. From Table 5, γ_2 is large value of 112. This indicats that the pore shape in this range are extremely flat. γ_3 is 1.54. This indicats that the pore shape in this range is nearly circular. It is considered that the pores in range i=2 is capillary pores and that their shape is a collapsed elliptic. The pores in range i=3 is entrained air and their shape is spherical. It is considered that the calculation result of γ_i expresses the pore shape properly and is qualitatively adequate.

4.3 Coefficients in micro cracking development law

The micro cracking development law is based theoretically on stress-dependent rate process theory. Therefore, if assumptions in organizing the equations are adequate, the coefficients calculated through reverse analysis under one condition will apply to other conditions. Here α, β, η, n_1, n_2 are determined from typical experimental data N-50-3-1.2.

The input data are shown in Table 6. The typical value C_2 in the pore volume increase range is 0.707 μ m which is the geometrical central value from 0.1 to 5 μ m.
$\rho_2(t)$ is estimated from test results of pore volume in N-50-3-1.2. The relationship with age and 0.1~5 μ m pore volume is shown in Fig.13. The time dependence of pore volume $V_2(t)$ is approximated by a hypabola. $\rho_2(t)$ is given by equation (24)

$$\rho_2(t) = V_2(t)\frac{2}{\pi\gamma_2 c_2{}^2} \tag{24}$$

A recurrent equation of tensile creep in N-50-3-1.2 and equation (24) are substituted for equation (12). $A_2(t\text{-}t')$ is in reverse analysis by time step 1 day. The five coefficients are given by these results. The reverse analysis result for $A_2(t\text{-}t')$ is shown in Fig.14. The coefficients of micro cracking development law are shown in Table 7.

In an experimental study of surface energy η, Hori[16] estimated the surface energy of hydrated cement paste from the relation between bending strength of hardened cement paste soaked in several liquids and the surface tension of the liquids . As a result, the surface energy γ of hydrated cement paste was expressed as $0.300 \sim 0.350 J/m^2$. However γ calculated in this study is larger than Hori's result by one order. In practice, it is considered that apparent γ is larger under the influence of aggregates and complicated crack shape. So it is considered that this difference is adequate. β including activity free energy ΔF which is another important physical coefficient will be investigated in the next chapter.

5. Verification of the prediction model

The prediction model for tensile creep presented in this study has been built up from the micro-level mechanism and fracture mechanics. The coefficients have been determined from restricted experimental results. The next step is to compare the results given by the prediction model with experiments under various test conditions. Temperature effects, we investigated to some extent based on a past study.

5.1 Outline of Experiments

Materials, specimens, and experimental methods were similar to those in Section 2. The experimental test series are shown in Table 8. Loading ages 7, 28, and 100 days and water cement ratio 40%, 60% were added to the parameters used in Section 2.

Table 8 Summary of Test Program

W/C (%)	Loading age (day)	Loading stress (N/mm^2)	Stress/ strength ratio	Loading duration (day)	Temp. (℃)	Humidity (%)
40	3	1.2	0.55	0,7,28	20	100 (Sealed)
50	3	0.8	0.29			
		1.2	0.52			
		1.6	0.63			
	7	1.2	0.40			
	28		0.39			
	180		0.34			
60	3	1.2	0.65			

Experiments in section 2

Table 9 Mix Proportions of Concrete

Type of cement	Gmax (mm)	Slump (cm)	Air (%)	W/C (%)	s/a (%)	unit weight(kg/m^3) W	C	S	G	ad. C×%
Normal	20	8±1	4.5±1	40	43.0	165	412	756	1011	0.25
				60	46.0	163	272	821	1025	

ad.:Air-entraining admixture

5.2 Test Results and Investigation

The input values used in the prediction model are shown in Table 10. The time dependence of pore volume $V_2(t)$ were approximated by hyperbola from unloaded specimens. $\rho_2(t)$ were calculated using equation (24) based on $V_2(t)$.

a) Effect of loading stress

In this test series, the loading age was fixed of 3 days and loading stress was changed. A comparison of the prediction model and experimental values is shown in Fig.15. Calculated loading stress, $0.8N/mm^2$, was smaller than the experimental value at ages below 15 days. Thereafter, the calculations accorded with the experimental value. On the other hand, the calculated loading stress, $1.6N/mm^2$, was smaller than the experimental value at ages greater than 10 days. But the calculations were in accord on earlier ages. The reasons for these differences are rather more likely related to the precision of $\rho_2(t)$ than to errors in assumptions. Anyway, the differences between calculations and experiments were few. It is concluded that the proposed

Table 10 Input Values

	effect of loading stress			effect of loading age			effect of W/C	
	N-50-3-0.8	N-50-3-1.2	N-50-3-1.6	N-50-7-1.2	N-50-28-1.2	N-50-180-1.2	N-40-3-1.2	N-60-3-1.2
$V_2(t)$	$\frac{0.0118t+0.0811}{5.703t}$	$\frac{0.0086t+0.1359}{4.896t}$	$\frac{0.0086t+0.1359}{4.896t}$	$\frac{-0.0011t+0.1516}{4.653t}$	$\frac{-0.0006t+0.1913}{5.538t}$	$\frac{0.0003t+0.1790}{5.262t}$	$\frac{0.0006t+0.1421}{4.993t}$	$\frac{0.0152t+0.1165}{4.940t}$
σ_y (N/mm^2)	0.8	1.2	1.6	1.2				
a_2 (mm)	0.0792							
γ_2	112							
E' (kN/mm^2)	58.7						58.7	58.0
α ($J/N/mm^2$)	0.0029							
β (1/s)	0.1955							
γ (J/mm^2)	2.5184							
$\frac{1}{n_1 kT}$ (1/J)	0.4850							
$\frac{1}{n_2 kT}$ (1/J)	0.9398							

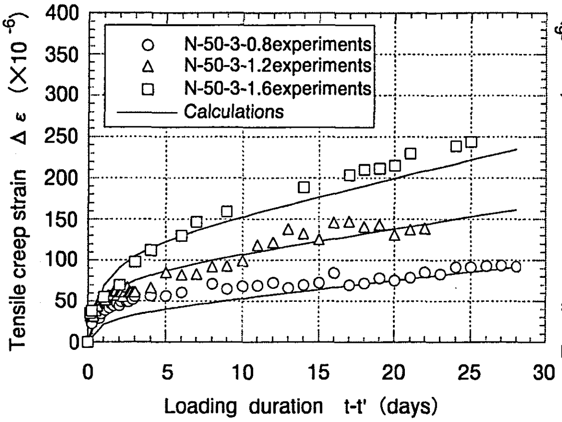

Fig.15 Experiments and Calculations

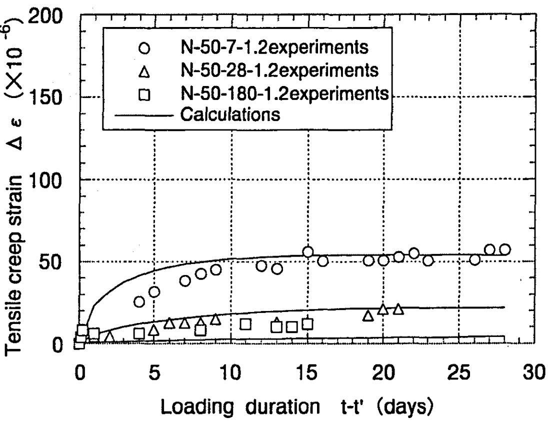

Fig.16 Experiments and Calculations

model successfully predicts tensile creep strains on the whole.

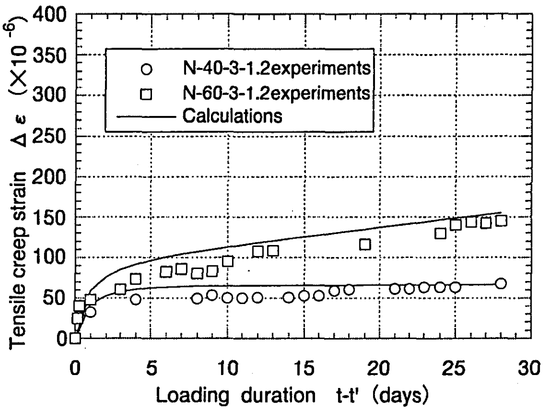

Fig.17 Experiments and Calculations

The calculations generally accord with experiments for stress/strength ratio from 0.29 to 0.63. When the stress/strength ratio is larger than in this study, calculations may diverge from experiments. Young[18] reported that limit of tensile creep strength exists at a stress/strength ratio of 0.6 ~ 0.7. Beyond this range, micro cracks will accumulate and localize, and macro cracks will develop (instability development). It is considered that creep strain rate will grow rapidly and the specimen will suffer creep fracture. However the prediction model proposed in this study is based on the stable development of micro cracks by repeated arrest and development. Namely, when macro crack growth is unstable, experimental values are larger than this prediction model. It is a very important theme that the phenomenon which micro cracks are accumulated, localized and developed to macro crack is predicted. Because it is related to predicting the cracking of structure. Currently the model cannot be treat this problem, so it must be extended in the future.

b) Effect of loading age
In this test series, loading stress was fixed at 1.2N/mm^2 and the loading age was changed. A comparison between calculations and experiments is shown in Fig.16. The calculations for a loading age of 7 days are a little larger than experimental values earlier in the loading. However, the calculations for loading ages of 28 and 180 days accorded with the experiments. The reasons for this difference are similar to those for loading stress and depend on the precision of $\rho_2(t)$. However, the discrepancy is little and it is considered that the model is able to predict changes in loading.

c) Effect of water cement ratio
In this test series, the loading stress was fixed at 1.2N/mm^2 and the loading age was fixed at 3 days. The Water-cement ratio was varied from 0.4 to 0.6. In the proposed prediction model, when mix proportion is changed, The Young's modulus of elastic frame E' must be changed. Then E' is recalculated using equation (23) for each mix proportion.

A comparison of calculations and experiments is shown in Fig.17. The calculations gave larger results than the experiments for all water-cement ratios. The reasons for this difference are similar to those discussed above; that is, it depends on the precision of $\rho_2(t)$. However, the discrepancies are few and it is considered that the model is able to predict changes in water-cement ratio.

d) Effect of temperature
The temperature has an effect on the creep strain of concrete. Generally, as temperature moves higher, the

Table 11 Input Values

	ΔF (J)		
	1×10^{-20}	5×10^{-20}	1×10^{-19}
σ_y (N/mm^2)	1.2		
a_2 (mm)	0.0792		
γ_2	112		
E' (kN/mm^2)	58.7		
α (J/N/m^2)	6.385×10^{-8}		
β (m/day)	1.190×10^{-7}	1.807×10^{-7}	3.980×10^{-7}
η (J/m^2)	5.8390		
$\frac{1}{n_1 kT}$ (1/J)	0.4540		
$\frac{1}{n_2 kT}$ (1/J)	0.8797		

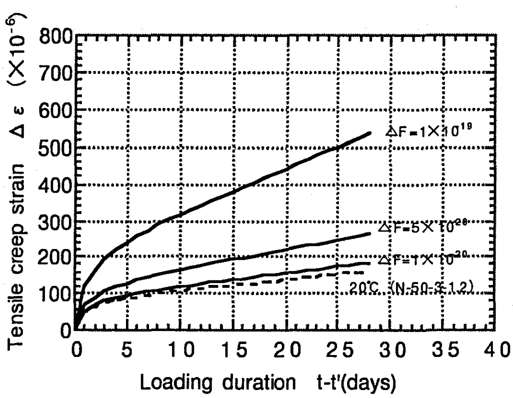

Fig.18 Parameter Analysis for Temperature

creep strain increases. An experimental study in which the loading age was fixedat three days and the temperature was changed has been carried out by Nomura and Umehara et al [17]. In their study, the tensile creep strain at 40℃ was about 1.5 times that at 20℃ after loading for 5days.

In the proposed prediction model for tensile creep strain, an absolute temperature term is included in the micro crack development law, as shown in equation (18). But in this study, β including unknown factor C and ΔF is coefficient at 20℃, so this model cannot express a temperature dependence. So, an analysis which is changed ΔF was carried out and the result was compared with Nomura and Umehara's result.

If the free active energy for fracturing a solid has a similar order to the free active energy of solidification, then ΔF is $10^{-19} \sim 10^{-20}$J. C is determined and $A_2(t\text{-}t')$ of N-50-3-1.2 is calculated. Input data are shown in Table 11. The micro crack development law $\rho_2(t)$ at 20℃ is adequate.

The result of parameter analysis are shown in Fig.18. The tensile creep strain at 40℃ changes with ΔF. If it is assumed that ΔF is about 5×10^{-19}J, then the result may accord with Nomura and Umehara's result. However, $\rho_2(t)$ at 20℃ is adequated in this study and it is expected that $\rho_2(t)$ at 40℃ would be smaller than that at 20℃ as a result of the hydration progress. The propriety of ΔF for predicting $\rho_2(t)$ at 40℃ must be discussed.

A characteristic of this model is that the tensile creep strain is given by a change in micro structure as $\rho_2(t)$ and micro crack development $A_2(t\text{-}t')$. When $\rho_2(t)$ and ΔF in the micro crack development law are evaluated appropriately, it is considered that the temperature effect of tensile creep may be predicted.

6. CONCLUSIONS

(1) A sustained tensile stress leads to an increase in micro pore volume in the 0.1 to 5 μ m pore diameter range. It is inferred that this increase must be due to the occurrence and development of micro cracks.

(2) The relationship between the increase in micro pore volume in the 0.1 to 5 μ m range and tensile creep strain is linear.

(3) It is assumed that the mechanism of tensile creep is that micro cracks occur and develop at capillary pores. A prediction model for tensile creep has been proposed based on physical theories such as fracture mechanics and the stress-dependent rate process theory.

(4) By comparing calculations by the prediction model against experiments under various test conditions. It is concluded that the model is able to predict tensile creep strain under changing loading stress, loading age, and water-cement ratio. However, when micro cracks accumulate, localize, and develop into macro cracks at the stress/strength ratios over 0.6 ~ 0.7, the prediction model may not be suitable.

(5) The ability of the model to handle temperature effects was investigated by looking at experimental data

from a past study. It was shown that the model may predict temperature effects on tensile creep strain while estimating the time dependence of the pore structure at high temperatures.

Acknowledgment
We wish to thank Mr. Tamotsu Kuroda, assistant in the Department of Civil Engineering at Tottori University , and students in the Department of Civil Engineering at Tottori University, for their assistance in the experimental work presented in this study. We express our sincere gratitude to them.

References

[1]Sakata, K.,"The Prediction of Shrinkage and Creep of Concrete", Concrete Journal, Vol.31, No2, pp.5-13, 1993 (in Japanese)
[2]Morimoto, H., Iwamoto, T., Kurihara N., and Koyanagi, W.,"The Characteristic of the Compressive and the Tensile Creep of Concrete at Early Ages", JCA Proc. of Cement and Concrete, No.47, pp.356-359, 1993 (in Japanese)
[3]Ward, M.A., and Cook, D.J.," The Mechanism of Tensile Creep in Concrete", Magazine of Concrete Research, Vol.21, No.68, pp.151-158, 1969
[4]Maekawa, K., Kishi, T., and Okamura, H., "The Transition of Required Performance and Designe Method of Cement and Concrete", Cement and Concrete, No.594, pp.2-9, 1996 (in Japanese)
[5]Kumano, T., Nishibayashi, S., and Kuroda, T.,"Effect of Tensile Stress on Microstructure of Concrete", JCA Proc. of Cement and Concrete, No.51, pp.818-823, 1997 (in Japanese)
[6]Hanehara, S.," The Structure and the Properties of Concrete", The Plain Cement Chemicals, No.9, JCA, pp.78-104, 1993 (in Japanese)
[7]Uchikawa, H.," Influence of Interfacial Structure between Cement Paste and Aggregate on the Quality of Hardened Concrete", Concrete Journal, Vol.33, No9, pp.5-17, 1995 (in Japanese)
[8]Tanaka, T., Tazawa, E., and Yonekura, A.," A Study on Mechanism of Tensile Creep of Concrete", Proc. of JSCE, No.42/V, pp.358-359, 1987 (in Japanese)
[9]JCI Committee for Studies on Analysis of Reaction Model," Report of Studies on Analysis of Reaction Model (1)", pp.162-163 (in Japanese)
[10]Kumano, T., Nishibayashi, S., and Inoue, S.," A Tensile Creep Model Based on Micro crack Behavior", Proc. of JSCE, No.52/V, pp.1040-1041, 1997 (in Japanese)
[11]Okamura, H.," Fracture Mechanics and Mterial Strength (1), A Introduction of Linear Fracture Mechanics", Baihukan, pp.120-123, 1976 (in Japanese)
[12]Yokohori, T.," Material Strength", Gihodo-shuppan, pp.10-14, 1956 (in Japanese)
[13]Mihashi, H.," A Stochastic Theory for Fracture of Concrete", Fracture Mechanics of Concrete, Elsevier Science Publishers B.V., pp.301-339, 1989
[14]Neville, A.M.," Characteristic of Concrete", Gihodo-shuppan, pp.219-226, 1979 (in Japanese)
[15]Soroka, I., and Sereda, P.J.," The Structure of Cement Stone and Use of Compacts as Structual Models", Proceeding the 5th International symposium on Chemical of Cement, Tokyo, Vol.III, pp.67-73, 1968
[16]Hori, M.," Strength of Hardened Cement Paste from view of Surface Energy", Ceramic Industry Association, Vol.70, No.7, pp.67-73, 1968 (in Japanese)
[17]Nomura, Y., Uehara, T., and Umehara, H.," A Study on Thermal Stress of Mass Concrete Considering Creep", Proc. of JCI, Vol.13, No.1, pp.845-850, 1991 (in Japnese)
[18]Al-Kubaisy, M.A., and Young, A.G.," Failure of Concrete under Sustained Tension", Magazine of Concrete Research, Vol.27, No.92, pp.171-178, 1975 (in Japanese)
[19]Iwasaki, K.," Characteristic of Concrete", Kyoritu-syuppan, pp.55-80, 1975 (in Japanese)
[20]Murata, J., and Okada, K.," The Newest Concrete Technology 1, Rheology of Fresh Concrete, Elastisity and Creep of Concrete", Sankaido, pp.139-143, 1970 (in Japanese)
[21]National Astronomic Observatory," Chronological Scientific Tables 1998", No.71, Maruzen, pp.143-144, 1997 (in Japanese)